



**Numerical Methods for Analysis of Charged Vacancy
Diffusion in Dielectric Solids**

**by John D. Clayton, Peter W. Chung, Michael A. Greenfield,
and William D. Nothwang**

ARL-TR-4002

December 2006

NOTICES

Disclaimers

The findings in this report are not to be construed as an official Department of the Army position unless so designated by other authorized documents.

Citation of manufacturer's or trade names does not constitute an official endorsement or approval of the use thereof.

Destroy this report when it is no longer needed. Do not return it to the originator.

Army Research Laboratory

Aberdeen Proving Ground, MD 21005-5066

ARL-TR-4002

December 2006

Numerical Methods for Analysis of Charged Vacancy Diffusion in Dielectric Solids

John D. Clayton, Michael A. Greenfield, and William D. Nothwang
Weapons and Materials Research Directorate, ARL

Peter W. Chung
Computational and Information Sciences Directorate, ARL

REPORT DOCUMENTATION PAGE			<i>Form Approved</i> OMB No. 0704-0188		
Public reporting burden for this collection of information is estimated to average 1 hour per response, including the time for reviewing instructions, searching existing data sources, gathering and maintaining the data needed, and completing and reviewing the collection information. Send comments regarding this burden estimate or any other aspect of this collection of information, including suggestions for reducing the burden, to Department of Defense, Washington Headquarters Services, Directorate for Information Operations and Reports (0704-0188), 1215 Jefferson Davis Highway, Suite 1204, Arlington, VA 22202-4302. Respondents should be aware that notwithstanding any other provision of law, no person shall be subject to any penalty for failing to comply with a collection of information if it does not display a currently valid OMB control number. PLEASE DO NOT RETURN YOUR FORM TO THE ABOVE ADDRESS.					
1. REPORT DATE (DD-MM-YYYY) December 2006		2. REPORT TYPE Final		3. DATES COVERED (From - To) October 2005–October 2006	
4. TITLE AND SUBTITLE Numerical Methods for Analysis of Charged Vacancy Diffusion in Dielectric Solids				5a. CONTRACT NUMBER	
				5b. GRANT NUMBER	
				5c. PROGRAM ELEMENT NUMBER	
6. AUTHOR(S) John D. Clayton, Peter W. Chung, Michael A. Greenfield, and William D. Nothwang				5d. PROJECT NUMBER FY06WMR15	
				5e. TASK NUMBER	
				5f. WORK UNIT NUMBER	
7. PERFORMING ORGANIZATION NAME(S) AND ADDRESS(ES) U.S. Army Research Laboratory ATTN: AMSRD-ARL-WM-TA Aberdeen Proving Ground, MD 21005-5066				8. PERFORMING ORGANIZATION REPORT NUMBER ARL-TR-4002	
9. SPONSORING/MONITORING AGENCY NAME(S) AND ADDRESS(ES)				10. SPONSOR/MONITOR'S ACRONYM(S)	
				11. SPONSOR/MONITOR'S REPORT NUMBER(S)	
12. DISTRIBUTION/AVAILABILITY STATEMENT Approved for public release; distribution is unlimited.					
13. SUPPLEMENTARY NOTES					
14. ABSTRACT A theory for charged vacancy diffusion in elastic dielectric materials is formulated and implemented numerically in a finite difference code. The governing equations consist of Maxwell's equations of electrostatics coupled with kinetic equations for vacancy diffusion, with the chemical potential accounting for both mixing energy of vacancies and electrostatically-driven charge migration. A second-order accurate implicit scheme is used to solve Maxwell's parabolic equations, while an explicit method is used to integrate the elliptic evolution equations for transient vacancy concentration. In addition to the theoretical background and numerical methodology, user documentation is included for the computer implementation, presently limited to one-dimensional analysis. Provided here are descriptions of the code structure, user instructions, and a representative application of the software for analysis of barium strontium titanate thin films containing charged oxygen vacancies. The source code is included in the appendix.					
15. SUBJECT TERMS thin films, dielectrics, electromechanics, diffusion					
16. SECURITY CLASSIFICATION OF:			17. LIMITATION OF ABSTRACT UL	18. NUMBER OF PAGES 40	19a. NAME OF RESPONSIBLE PERSON John Clayton
a. REPORT UNCLASSIFIED	b. ABSTRACT UNCLASSIFIED	c. THIS PAGE UNCLASSIFIED			19b. TELEPHONE NUMBER (Include area code) 410-306-0975

Contents

List of Figures	iv
List of Tables	iv
1. Introduction	1
2. Theory	2
2.1 Model Framework	2
2.2 One-Dimensional Model	5
3. Numerical Methods	7
3.1 Electrostatics	7
3.2 Transient Diffusion.....	8
4. Software Manual	10
4.1 Code Structure.....	10
4.2 Input.....	11
4.3 Output.....	13
5. Sample Problem-BST Film	14
6. Conclusions	17
7. References	18
Appendix. Source Code	19
Distribution List	33

List of Figures

Figure 1. One-dimensional problem domain.	5
Figure 2. Spatial discretization.	7
Figure 3. Flowchart for code execution.	11
Figure 4. Vacancy concentration and electric field: $c_0 = 1$ ppm , $V = 0$	16

List of Tables

Table 1. Properties of BST film at 298 K.	14
--	----

1. Introduction

Dielectric materials with charged defects exhibit a variety of physical phenomena whose origins are not fully understood. Early continuum theories (Devonshire, 1954; Toupin, 1956) of the electromechanical behavior of dielectric media have been set forth, though these do not consider defects explicitly. However, defects such as vacancies have been the focus of considerable study (Lifshitz, 1963), particularly with regards to crystalline ceramics of current interest to the U.S. Army Research Laboratory.

The unique aspect of the present study is consideration of electrically charged, as opposed to neutral, vacancies in dielectric solids. Defect concentrations and excess charges in ferroic ceramics may be adjusted during processing via heat treatments and/or addition of doping chemicals (Cole et al., 2003). Charged point defects have been identified as a major factor affecting the reliability of ferroelectric devices (Damjanovic, 1998), including gate dielectric semiconductors, particularly those of thin film geometry (Buchanan, 1999).

Here, a general modeling framework is constructed for elastic dielectric semiconductors with mobile charged point vacancies. This framework combines the physics of continuum elasticity, electrostatics, mass diffusion, and charged defect kinetics. Changes in surface morphology due to the boundary flux of charged vacancies are captured, extending a previous theory of one of the co-authors on neutral vacancy kinetics (Grinfeld and Hazzledine, 1997).

The theory is implemented numerically in a finite difference code (Hoffman, 1992) enabling simultaneous solution of the elliptic equations of electrostatics of dielectrics and the transient parabolic equations of charged diffusion. The analysis is limited to a single spatial dimension. The time duration of the problem is decomposed into a sequence of steps. A second-order accurate fully implicit scheme is invoked to solve Maxwell's equations in each step, while a fully explicit scheme is used to integrate the transient vacancy concentration. The spatial domain and grid spacing are updated when the surface flux of concentration is nonzero, as vacancies exiting the domain influence its instantaneous dimensions.

Documentation is presented for the computer implementation. Included here are descriptions of the source code structure, user instructions, and representative input files for the software, the latter specifically for analysis of barium strontium titanate ($\text{Ba}_{1-x}\text{Sr}_x\text{TiO}_3$) (BST) thin films containing charged oxygen vacancies. The source code is given in the appendix.

In the notation that follows, the Einstein summation convention is used on repeated lower-case indices, unless indicated otherwise. Cartesian spatial coordinate indices span three dimensions and are written in Roman font, while curvilinear surface coordinate indices span two dimensions

and are written in Greek font. Subscripted commas denote covariant differentiation. Capitalized subscripts are often used in physical constants and are not summed. In the description of numerical methods, subscripts are often used for node numbers, and superscripts for time increments.

2. Theory

The governing equations, thermodynamic framework, and constitutive relations are first presented, with limited derivations, in three-dimensional (3-D) form in section 2.1. The one-dimensional (1-D) equations that are solved numerically follow in section 2.2.

2.1 Model Framework

The local electrostatic behavior of dielectric continua is dictated by Maxwell's equations (Stratton, 1941):

$$D_{,i}^i = \hat{\rho}, \quad (1)$$

$$E_i = -\phi_{,i}, \quad (2)$$

and

$$D^i = \varepsilon_0 E^i + P^i, \quad (3)$$

where D is the electric displacement, $\hat{\rho}$ is the charge density, E is the electric field, ϕ is the electrostatic potential, and ε_0 is the permittivity of free space. The polarization vector P is defined only within the material and vanishes in free space. Local mechanical equilibrium and mass conservation are ensured by

$$\sigma_{,j}^{ij} = 0 \quad (4)$$

and

$$\dot{\rho} + \rho u_{,i}^i = 0, \quad (5)$$

where σ is the symmetric Cauchy stress, ρ is the mass density of the deformed solid with vacancies, and u is the displacement, which itself encompasses expansion or contraction due to vacancies within the bulk material. Small displacements are assumed henceforth in the present theory. The balance of energy and the dissipation inequality may be written in global rate form as

$$\Phi = W - \dot{\Omega} \geq 0, \quad (6)$$

with Φ the dissipation, W the rate of external work, and Ω the system energy. For a dielectric solid containing mobile charged vacancies, the external work and energy of the system are

$$W = \frac{d}{dt} \int \hat{\sigma} \phi ds + \int \hat{t}^i u_i ds - \int \mu Q^i n_i ds \quad (7)$$

and

$$\dot{\Omega} = \int \rho (\dot{U} - \theta \dot{\eta}) dv + \frac{d}{dt} \int (1/2) \epsilon_0 |\phi_{,i}|^2 dv + \frac{d}{dt} \int \hat{\sigma} \phi ds, \quad (8)$$

where s and v are the surface and volume of the system with unit normal n , $\hat{\sigma}$ is the surface charge density, \hat{t} is the traction vector, μ is the chemical potential for vacancy diffusion, Q is the vacancy flux, U is the internal energy per unit mass of the substance, and γ is the surface energy density. Heat conduction is not considered explicitly here, as is evident from equations 6–8. The Helmholtz free energy ψ , specific entropy η , and temperature θ are related by the usual thermodynamic relationship

$$\psi = U - \eta \theta. \quad (9)$$

The following constitutive assumptions are made regarding the free energy and charge density:

$$\psi = \psi(u_{i,j}, P^i, \theta, \xi), \quad (10)$$

and

$$\hat{\rho} = ez\xi, \quad (11)$$

where ξ is the number of vacancies per unit volume. Assumption (equation 10) suggests a free energy dependence on mechanical strain, polarization, temperature, and vacancy concentration. Equation 11 denotes that the charge density is proportionate to the vacancy concentration, with e and z the charge of an electron and the valence contribution of each defect, respectively. Substituting equations 9–11 into equation 6 and making use of the balance laws in equations 1–5 and the divergence theorem, and restricting $\dot{\phi} = 0$ on s , the following thermodynamically admissible bulk constitutive relations may be derived:

$$E_i = \rho \partial \psi / \partial P^i, \quad (12)$$

$$\sigma^{ij} = \rho \partial \psi / \partial u_{i,j}, \quad (13)$$

$$\eta = -\partial \psi / \partial \theta, \quad (14)$$

$$\dot{\xi} = -Q^i_{,i}, \quad (15)$$

$$Q^i = -d^{ij} \mu_{,j}, \quad (16)$$

and

$$\mu = \rho \partial \psi / \partial \xi + ez\phi, \quad (17)$$

where the diffusivity tensor d is symmetric and positive definite. Let $\chi = \alpha\xi$ denote the volume fraction of vacancies, with α is a scalar conversion factor. Mass conservation requires that

$$\dot{a}(1-\chi) = -\alpha(Q^i n_i + q_{,\alpha}^\alpha), \quad (18)$$

where \dot{a} is the surface velocity of the substance with unit normal n and q is the flux tangential to the surface of charged vacancies. Conservation of mechanical work leads to

$$\hat{t}^i = \rho \partial \psi / \partial u_{i,j} n_j. \quad (19)$$

By requiring that the volumetric energy of the system Ω remain constant or decrease with time in the absence of mechanical working due to external stresses, the following relations for the in-plane and normal surface fluxes are formulated:

$$q^\alpha = A^{\alpha\beta} \left((\rho\psi + \hat{\rho}\phi\chi) / (1-\chi) \right)_{,\beta}, \quad (20)$$

and

$$(1-\chi)Q^i n_i = \beta \left(\rho\psi + \hat{\rho}\phi + (1-\chi) \left(\rho \partial \psi / \partial \chi + \alpha^{-1} e z \phi \right) \right), \quad (21)$$

where A is the symmetric positive definite surface diffusivity tensor and β is a positive scalar characterizing the resistance of the surface to penetration by vacancies. Implicit in equations 4, 13, and 19 is the vanishing of Maxwell's stress tensor (Toupin, 1956), meaning that contributions from terms of second order in the electric field and polarization are neglected in the mechanical equilibrium equations.

The continuum theory is applied here to describe linear elastic dielectric solids. A specific form of the free energy density is thus postulated as

$$\rho\psi = (1/2) \mathbb{C}^{ijkl} u_{(i,k)} u_{(j,l)} + (1/2) \lambda_{ij} P^i P^j + \varphi(\xi, \theta), \quad (22)$$

where \mathbb{C} and λ are linear-elastic moduli and inverse dielectric susceptibility, respectively, and symmetrized indices are in parentheses. Presently, we address only the response of the material in its paraelectric state, at temperatures above the Curie point. Thus, phase transformations, piezoelectricity, pyroelectricity, and spontaneous polarization are not considered. From equation 22, bulk thermodynamic relations in equations 12, 13, and 3 reduce to

$$\sigma^{ij} = \mathbb{C}^{ijkl} u_{(k,l)}, \quad (23)$$

$$E_i = \lambda_{ij} P^j, \quad (24)$$

and

$$D^i = \varepsilon_0 \varepsilon_R^{ij} E_j, \quad (25)$$

with $\varepsilon_R^{ij} = \delta^{ij} + \varepsilon_0^{-1} \lambda^{-1ij}$ the relative permittivity (i.e., real dielectric constant). The vacancy and temperature-dependent contribution φ is assumed here to follow the universal relation for the chemical potential of an ideal mixture (Fried et al., 1977), most relevant for noninteracting species and small vacancy concentrations:

$$\varphi N_A = N_T (G_0(\theta) + N_A k_B \theta \nu \ln \nu). \quad (26)$$

In equation 26, N_A is Avagadro's number, k_B is Boltzmann's constant, $N_T = 1/\alpha$ is the number of atomic sites per unit volume, ν is the mole fraction of vacancies, and G_0 is the bulk Gibbs free energy of unstressed, defect-free substance. As implemented here, we assume simply that

$$G_0 = \theta [\hat{c}(\theta) - \hat{\eta}(\theta)], \quad (27)$$

with specific heat \hat{c} and specific entropy $\hat{\eta}$. Upon application of equation 26, the kinetic equation for bulk diffusion then follows directly from equation 16 as

$$Q^i = -d^{ij} (k_B \theta \chi_{,j} / \chi - e z E_j). \quad (28)$$

2.2 One-Dimensional Model

The physical system analyzed is a substance of length (i.e., thickness) T with applied bias voltage V , as shown in figure 1. Alternatively to voltage boundary conditions, electric fields may be applied at the boundaries (not shown in figure 1). No mechanical tractions are applied, and isotropic material properties are assumed ($\varepsilon_R^{ij} = \varepsilon_R \delta^{ij}$, $d^{ij} = d \delta^{ij}$), thus rendering the analysis one dimensional in thickness direction x . Correspondingly in this analysis, surface flux $q^\alpha = 0$ and surface tension $\tau = 0$. A constant temperature θ is assumed.

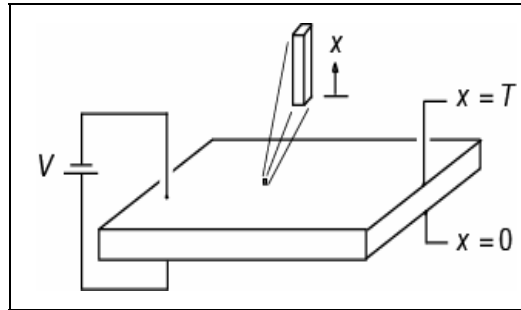


Figure 1. One-dimensional problem domain.

Under the preceding conditions, the governing electrostatic equations 1–3 reduce to

$$dD/dx = \varepsilon_0 \varepsilon_R dE/dx = -\varepsilon_0 \varepsilon_R (d^2 \phi / dx^2) = \hat{\rho}. \quad (29)$$

The vacancy evolution equations 28 and 15 become

$$Q = -d(k_B\theta/\chi(d\chi/dx) - ezE) \quad (30)$$

and

$$\dot{\chi} = -\alpha(dQ/dx), \quad (31)$$

with the domain size evolving, from equation 18, as

$$\dot{a} = \alpha(Q(T)/(1-\chi(T)) - Q(0)/(1-\chi(0))). \quad (32)$$

Spatial boundary conditions are applied as follows:

$$\hat{t}(0,t) = \hat{t}(L,t) = 0, \quad (33)$$

$$\phi(0,t) = V_0 \quad \text{or} \quad E(0,t) = E_0, \quad (34)$$

$$\phi(T,t) = V_T \quad \text{or} \quad E(T,t) = E_T, \quad (35)$$

$$\chi(0,t) = \chi_0 \quad \text{or} \quad Q(0,t) = Q_0, \quad (36)$$

and

$$\chi(T,t) = \chi_T \quad \text{or} \quad Q(T,t) = Q_T. \quad (37)$$

The boundary fluxes Q_0 and Q_T may be prescribed as constant values, or determined instantaneously from the model thermodynamics (equation 21):

$$(1-\chi)Q = -\beta(\rho\psi + \hat{\rho}\phi + (1-\chi)(\rho\partial\psi/\partial\chi + \alpha^{-1}ez\phi)). \quad (38)$$

Initial conditions for the vacancy concentration and electrostatic charge density are applied as

$$\chi(x,0) = \bar{\chi}(x) \quad (39)$$

and

$$\hat{\rho}(x,0) = \bar{\rho}(x), \quad (40)$$

where $\bar{\rho} = ez\bar{\chi}/\alpha$ should be imposed for consistency with equation 11.

Note from equations 30 and 31 that the electric field may act as a local source or sink for vacancies, implying that ions may be impinged within or released from the lattice due to electrostatic forces. In some cases, it is convenient and realistic to impose an additional constraint that the total number of vacancies in the system remains constant, i.e.,

$$\int_0^T \chi dx = \bar{\chi}_0 T, \quad (41)$$

where $\bar{\chi}_0$ is the initial average concentration.

3. Numerical Methods

The time duration of the problem is decomposed into a series of steps. For each time step, the electrostatic problem is solved, with the corresponding solution for the electric field used in the transient equations (equation 30) for updating the vacancy concentration. In the following time step, this updated vacancy concentration is used to compute the local electric charge entering Maxwell's equations (equation 29). The analysis thus marches forward in time, with the numerical solutions of the equations of electrostatics and diffusion coupled in this manner.

The 1-D spatial domain is discretized into $n-1$ increments of equal length Δx , with n the total number of nodes, as shown in figure 2.

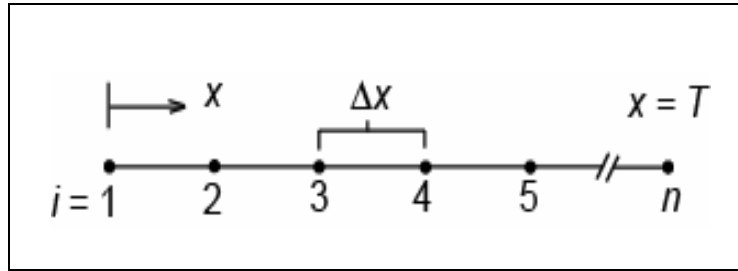


Figure 2. Spatial discretization.

3.1 Electrostatics

A second-order accurate implicit scheme is used to solve Maxwell's static equations in each step. Within the domain $0 < x < T$, equation 29 is written, to accuracy of order $(\Delta x)^2$, using a finite difference approximation (Hoffman, 1992) for the second spatial derivative of ϕ :

$$\phi_{i+1} - 2\phi_i + \phi_{i-1} = -\hat{\rho}_i (\Delta x)^2 / \epsilon_0 \epsilon_R, \quad (42)$$

where subscripts denote node numbers. The solution of equation 42 for all nodes i is then written in matrix form as

$$[\phi] = [\mathbf{A}]^{-1} [\rho], \quad (43)$$

where $[\phi]$ is the n -dimensional solution vector of nodal electric potentials, $[\mathbf{A}]$ is the $n \times n$ coefficient matrix that is generally tridiagonal and sparse, and $[\rho]$ is an n -dimensional vector that corresponds to the right hand side of equation 42. In the solution procedure, the dimensions of $[\phi]$, $[\mathbf{A}]$, and $[\rho]$ are reduced by one for each electrostatic potential boundary condition enforced a priori. Once the electric potential is known, the electric field is then computed numerically as

$$-2\Delta x E_i = \phi_{i+1} - \phi_{i-1}. \quad (44)$$

The following second-order finite difference approximations are used at the boundaries ($i = 1$ and $i = n$):

$$-2\Delta x E_1 = -3\phi_1 + 4\phi_2 - \phi_3, \quad (45)$$

and

$$-2\Delta x E_n = \phi_{n-2} - 4\phi_{n-1} + 3\phi_n. \quad (46)$$

3.2 Transient Diffusion

A fully explicit scheme is used to integrate the transient vacancy concentration, with all necessary spatial derivatives obtained using a second-order accurate finite difference approach. The vacancy flux (equation 30) is written as follows, where subscripts denote node numbers:

$$Q_i = -d \left(d(\rho \partial \psi / \partial \chi_i) / dx - e z E_i \right), \quad (47)$$

where for nodes in the domain $0 < x < T$,

$$\rho \partial \psi / \partial \chi_i = k_B \theta \ln \chi_i \quad (48)$$

and

$$d(\rho \partial \psi / \partial \chi_i) / dx = k_B \theta (\ln \chi_{i+1} - \ln \chi_{i-1}) / 2\Delta x. \quad (49)$$

Note that in equation 47, the electric field E_i is obtained from the electrostatic solution given by equations 44–46. At the boundaries, the following approximations were used, analogous to equations 45 and 46:

$$d(\rho \partial \psi / \partial \chi_1) / dx = k_B \theta (-\ln \chi_3 + 4 \ln \chi_2 - 3 \ln \chi_1) / 2\Delta x, \quad (50)$$

and

$$d(\rho \partial \psi / \partial \chi_n) / dx = k_B \theta (\ln \chi_{n-2} - 4 \ln \chi_{n-1} + 3 \ln \chi_n) / 2\Delta x. \quad (51)$$

The rate equation for concentration is approximated as follows for $0 < x < T$:

$$\dot{\chi}_i = -\alpha (Q_{i+1} - Q_{i-1}) / 2\Delta x, \quad (52)$$

and at the boundaries as

$$\dot{\chi}_1 = -\alpha (-Q_3 + 4Q_2 - 3Q_1) / 2\Delta x \quad (53)$$

and

$$\dot{\chi}_n = -\alpha (Q_{n-2} - 4Q_{n-1} + 3Q_n) / 2\Delta x. \quad (54)$$

Application of concentration boundary conditions simply entails $\dot{\chi}_i = 0$, while application of constant flux conditions at a boundary eliminates the need to solve (equation 47) at that

boundary. When transient flux conditions (equation 38) are applied, the following approximation suffices:

$$(1 - \chi_i) Q_i = -\beta \left(\rho \psi_i + \hat{\rho}_i \phi_i + (1 - \chi_i) k_B \theta \ln \chi_i + \alpha^{-1} e z \phi_i \right), \quad (55)$$

where the free energy per unit volume is found from

$$\rho \psi_i = \varepsilon_0 \varepsilon_R |E_i|^2 / 2 + N_T \left(G_0 + N_A k_B \theta \left(\chi_i / \alpha N_T \right) \ln \left(\chi_i / \alpha N_T \right) \right) / N_A. \quad (56)$$

Finally, the concentration is updated explicitly as

$$\chi_i^{t+\Delta t} = \chi_i^t + \dot{\chi}_i \Delta t, \quad (57)$$

where Δt is the time increment.

The logarithmic form of the chemical potential, and flux equations 48–51, require that $\chi_i > 0$.

This is achieved in practice by enforcing

$$\dot{\chi}_i \rightarrow 0 \vee i \in \chi_i^{t+\Delta t} < \chi_{\min}, \quad (58)$$

where $\chi_i^{t+\Delta t}$ is the projected updated concentration from equation 57 and $\chi_{\min} = 10^{-21}$ is a near-negligible, default minimum concentration. Optional global conservation condition (equation 41) is imposed by rescaling equation 57:

$$\chi_i^{t+\Delta t} = \bar{\chi}_0 T \left(\chi_i^t + \dot{\chi}_i \Delta t \right) \left(\frac{n-1}{n} \Delta x \sum_{i=1}^n \left(\chi_i^t + \dot{\chi}_i \Delta t \right) \right)^{-1}. \quad (59)$$

The domain size is updated from equation 32 as

$$\dot{a} = -\alpha \left(Q_n / (1 - \chi_n) - Q_1 / (1 - \chi_1) \right) \quad (60)$$

and

$$\Delta x^{t+\Delta t} = (T + \dot{a} \Delta t) / (n - 1). \quad (61)$$

For the solution of equation 42 in the next time step, the updated charge concentration is found from equation 11:

$$\hat{\rho}_i^{t+\Delta t} = e z \chi_i^{t+\Delta t} / \alpha. \quad (62)$$

A fixed time increment is used throughout the analysis, i.e.,

$$\Delta t = t_{\max} / m, \quad (63)$$

where t_{\max} and m are the total simulation time and number of time increments, respectively.

Convergence and stability of the numerical solution dictate the practical choice of Δt

(Chapra and Canale, 1998). Let $\bar{D} = dk_B\theta / \xi_R$, where ξ_R is a reference concentration per unit volume, on the order of the minimum local concentration in the domain. Then one may write

$$\Delta t \leq \Lambda (\Delta x)^2 / \bar{D}, \quad (64)$$

where $\Lambda \leq 1/2$ guarantees convergence and stability. Setting $\Lambda \leq 1/4$ ensures that the solution will not oscillate, while the choice $\Lambda = 1/6$ has been shown, for the pure diffusion problem, to minimize truncation error (Carnahan et al., 1969). A description of what effect the unique electric field term ezE_i in equation 47 may have on stability and convergence is not presently available.

4. Software Manual

In what follows, the source code structure, input files, and output files are documented. Note that for reference, the complete code is contained in the appendix.

4.1 Code Structure

The source code is written in the standard FORTRAN90 language. It has been compiled with Portland Group's FORTRAN compiler (i.e., pgf90) (<http://www.pgroup.com/>) and executed on a 64-bit Linux workstation. Floating point values are represented in scientific double precision. This is a serial, as opposed to parallel, code. The program permits solution of the elliptic differential equations of electrostatics and/or the parabolic differential equations for transient diffusion. Standard SI units are used throughout. The software enables all of the features described in section 3, as well as a few additional options offering additional user flexibility. The code consists of the following routines:

- the main routine, 'semiconductor_1D', which controls the grid spacing, memory allocation, and time incrementation.
- subroutine 'elliptic', which solves Maxwell's equations.
- subroutine 'parabolic', which solves the transient diffusion equations.
- subroutine 'chem_potential', which computes the local free energy and its gradient.
- subroutine 'LU_decomp', which decomposes the $[\mathbf{A}]$ matrix in (43) to LU-form.
- subroutine 'LU_backsub', which solves equation 43 using a back substitution technique.

Figure 3 is a flowchart demonstrating execution of the code.

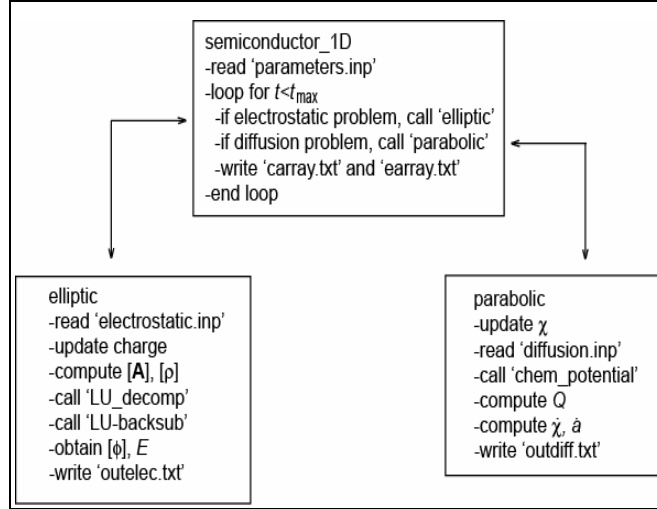


Figure 3. Flowchart for code execution.

4.2 Input

Up to three input files are required. The file read by the main routine, 'parameters.inp', is always required. Its format is as follows:

'parameters.inp'

Line 1: problem type. Specify 'maxwell' to solve only the electrostatic equations, 'fick' to solve only the diffusion equations, or 'mixed' to solve the fully coupled electrostatic-diffusion problem

Line 2: number of nodes n

Line 3: solution end time t_{\max} [s]

Line 4: fixed time increment Δt [s]

Line 5: number of time steps in between each write to the output files, n_t

Line 6: domain thickness T [m]

Line 7: temperature θ [K]

Line 8: relative dielectric permittivity $\epsilon_{R,0}$

Line 9: factor κ enabling permittivity to depend on local electric field (Johnson, 1962):

$$\epsilon_R = \epsilon_{R,0} \left(1 + \kappa E^2\right)^{-1/3}$$

Line 10: diffusivity d

Line 11: diffusivity \hat{d} for electrostatic contribution (set $\hat{d} = d$ for consistency with equation 47):

$$Q_i = -d \left(d \left(\rho \partial \psi / \partial \chi_i \right) / dx \right) + \hat{d} e z E_i$$

Line 12: factor for conversion of concentration from [ppm] to $[m^{-3}]$, equal to $10^{-6} / \alpha [m^{-3}]$

Line 13: factor for conversion of concentration from [ppm] to volume fraction, nominally 10^{-6}

Line 14: valence contribution per vacancy, z

Line 15: specific entropy $\hat{\eta}$ [J/mol K]

Line 16: specific heat capacity \hat{c} [J/mol K]

The file 'electrostatic.inp' is read only if the problem type is 'maxwell' or 'mixed'. Its format is specified as follows:

'electrostatic.inp'

Line 1: boundary condition at $x = 0$. Use 'potential' to supply a voltage ϕ , or 'flux' to supply an electric field E

Line 2: value of $\phi(x = 0)$ [V] for a 'potential' condition, or value of $E(x = 0)$ [V/m] for a 'flux' condition

Line 3: boundary condition at $x = T$. Use 'potential' to supply a voltage ϕ , or 'flux' to supply an electric field E

Line 4: value of $\phi(x = T)$ [V] for 'potential' condition, or value of $E(x = T)$ [V/m] for 'flux' condition

Line 5: text heading (not used)

Line 6: initial charge density at node 1, $\hat{\rho}_{i=1}^{t=0}$ [C/m³]

Line 7: initial charge density at node 2, $\hat{\rho}_{i=2}^{t=0}$ [C/m³]

·
·
·

Line $n + 5$: initial charge density at node n , $\hat{\rho}_{i=n}^{t=0}$ [C/m³]

The file 'diffusion.inp' is read only if the problem type is 'fick' or 'mixed'. Its format is given as follows:

'diffusion.inp'

Line 1: boundary condition at $x = 0$. Use 'potential' to supply a constant vacancy concentration c , 'flux' to supply a constant vacancy flux Q , or 'special' to apply equation 55.

Line 2: value of $c(x = 0)$ [ppm] for a 'potential' condition, value of $Q(x = 0)$ [ppm m/s] for a 'flux' condition, or value of β in (55) for 'special' condition

Line 3: boundary condition at $x = T$. Use 'potential' to supply a constant vacancy concentration c , 'flux' to supply a constant vacancy flux Q , or 'special' to apply equation 55.

Line 4: value of $c(x = T)$ [ppm] for a 'potential' condition, value of $Q(x = T)$ [ppm m/s] for a 'flux' condition, or value of β in (55) for 'special' condition

Line 5: flag to apply constraint (59): 'yes' or 'no'

Line 6: initial vacancy concentration at node 1, $c_{i=1}^{t=0}$ [ppm]

Line 7: initial vacancy concentration at node 2, $c_{i=2}^{t=0}$ [ppm]

·
·
·

Line $n + 5$: initial vacancy concentration at node n , $c_{i=n}^{t=0}$ [ppm]

4.3 Output

Up to four output files are generated, each containing computational results. The file 'outelec.txt' is written for problems of type 'maxwell' or 'mixed', and provides the following:

'outelec.txt'

At output request times $t = 0, t = t_{\max} / n_t, t = 2t_{\max} / n_t, \dots, t = (n_t - 1)t_{\max} / n_t, t = t_{\max} :$

Column 1: node i

Column 2: time t [s]

Column 3: position x [m]

Column 4: electric potential ϕ_i [V]

Column 5: electric field E_i [V/m]

Column 6: electric charge $\hat{\rho}_i$ [C/m³]

The file 'outdiff.txt' is written for problems of type 'fick' or 'mixed', and provides the following:

'outdiff.txt'

At output request times $t = 0, t = t_{\max} / n_t, t = 2t_{\max} / n_t, \dots, t = (n_t - 1)t_{\max} / n_t, t = t_{\max} :$

Column 1: node i

Column 2: time t [s]

Column 3: position x [m]

Column 4: vacancy concentration c [ppm]

Column 5: concentration rate \dot{c} [ppm/s]

Column 6: vacancy flux Q [ppm m/s]

The file 'earray.txt' contains the electric field data in tabular form for easy generation of 3-D mesh plots. Zeros are returned if the 'elliptic' routine is not called. The format is as follows:

'earray.txt'

Rows correspond to node numbers i , while columns correspond to time increments.

Column 1: x coordinate of each node i , at $t = t_{\max}$

Column 2: electric field E_i [kV/cm] at each node i , at $t = 0$

Column 3: electric field E_i [kV/cm] at each node i , at $t = t_{\max} / n_t$

.

.

.

Column $n_t + 2$: electric field E_i [kV/cm] at each node i , at $t = t_{\max}$

The file 'carray.txt' contains the vacancy concentration data in tabular form for easy generation of 3-D mesh plots. Zeros are returned if the 'parabolic' routine is not called. The format is listed as follows:

'carray.txt'

Rows correspond to node numbers i , while columns correspond to time increments.

Column 1: x coordinate of each node i , at $t = t_{\max}$

Column 2: concentration c_i [ppm] at each node i , at $t = 0$

Column 3: concentration c_i [ppm] at each node i , at $t = t_{\max} / n_t$

·
·
·

Column $n_t + 2$: concentration c_i [ppm] at each node i , at $t = t_{\max}$

5. Sample Problem-BST Film

An example problem is discussed here to demonstrate the software capabilities and input file format. The physical system analyzed here is a thin film of uniform thickness $T = 100$ nm (figure 1). Isothermal conditions are assumed with $\theta = 298$ K, a temperature at which undoped BST remains cubic in phase for molar concentrations of Sr greater than 0.3 (Tinte et al., 2004). Doping with Mg further lowers the Curie point (Cole et al., 2003).

Requisite material properties are listed in table 1, deemed representative of particular composition $\text{Ba}_{0.6}\text{Sr}_{0.4}\text{TiO}_3$. The dielectric constant ϵ_R is chosen as representative of the BST film systems of interest (Cole et al., 2003), while thermodynamic properties \hat{c} and $\hat{\eta}$ of the bulk substance are used (Todd and Lorenson, 1952). The vacancy diffusivity d is computed from

$$\bar{D} = \bar{\mu} k_B \theta / e z = d k_B \theta / \xi_R, \quad (65)$$

where \bar{D} is a thermally-activated diffusivity associated with Fick's first law, $\bar{\mu}$ is the drift mobility of ionic charges, and ξ_R is a reference defect concentration. We assume here, from drift mobility data on 100 nm-thick BST films (Zafar et al., 1998), a constant value of $\bar{\mu} \xi_R = 2(10)^{-8} \text{ V}^{-1} \text{ m}^{-1} \text{ s}^{-1}$, leading to the value of d reported in table 1. Parameter α is estimated from consideration of the crystal structure and lattice parameters, while the value of z indicates that each oxygen vacancy contributes a charge of magnitude of two free electrons.

Table 1. Properties of BST film at 298 K.

Parameter	Value	Parameter	Value
ϵ_R	500	d	$6.24(10)^{10} \text{ J}^{-1} \text{ m}^{-1} \text{ s}^{-1}$
\hat{c}	$100 \text{ J mol}^{-1} \text{ K}^{-1}$	α	10^{-29} m^3
$\hat{\eta}$	$115 \text{ J mol}^{-1} \text{ K}^{-1}$	z	2.0

The particular initial-boundary value problem includes the following boundary conditions, corresponding to shorted or ground electrodes at the film boundaries, which themselves are constrained to remain impenetrable to vacancy flow:

$$\phi(0,t) = 0, \quad \phi(T,t) = 0, \quad (66)$$

$$Q(0,t) = 0, \quad Q(T,t) = 0. \quad (67)$$

Initial conditions are applied as

$$\chi(x,0) = 10^{-6} \quad (68)$$

and

$$\hat{\rho}(x,0) = 32043 \text{ C/m}^3. \quad (69)$$

The spatially-constant value of $\chi(x,0) = 10^{-6}$ corresponds to an initial concentration of $c_0 = 1 \text{ ppm}$. Additionally, vacancy conservation constraint (59) is activated throughout the analysis. The spatial domain is decomposed into 300 segments of equal length $\Delta x = 1/3 \text{ nm}$, with a total of 301 nodes. The time domain is chosen as $0 \leq t \leq 1 \mu\text{s}$. Input files used for the computation are as follows:

'parameters.inp'

```
mixed
301
1.0d-6
1.0d-12
100000
1.0d-7
298
500
0.0
6.24d10
6.24d10
1.0d23
1.0d-6
2.0
115.0
100.0
```

'electrostatic.inp'

```
potential
0.0
potential
0.0
initial_charge_distribution
32043.0
32043.0
.
.
.
32043.0
```

```
'diffusion.inp'
```

```
flux  
0.0  
flux  
0.0  
yes  
1.0  
1.0  
. . .  
1.0  
1.0
```

The solution is shown in figure 4, with concentration and electric field mesh plots generated from output files 'carray.txt' and 'earray.txt', respectively. Although a steady-state concentration is not reached in the short duration of this transient simulation, a buildup of vacancies at the boundaries $x = 0$ and $x = T = 100$ nm occurs, as the charges migrate from their initially uniform distribution towards the boundaries where the voltage $\phi = 0$. Vacancy migration has a negligible effect on the local electric field E , however, which is initially linear due to the constant initial charge distribution and exhibits an average value of zero.

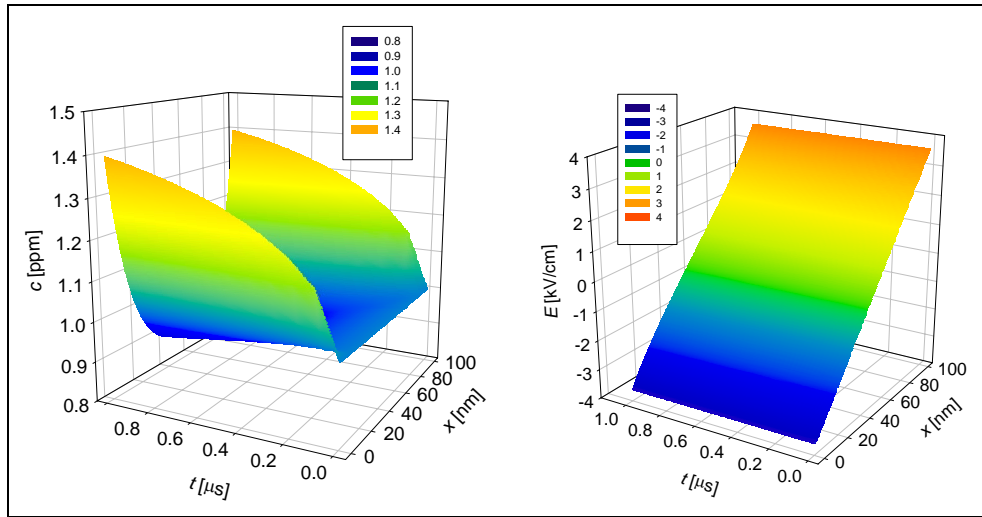


Figure 4. Vacancy concentration and electric field: $c_0 = 1$ ppm, $V = 0$.

Vacancy concentration distributions can be explained upon further examination of chemical potential μ of equation 17. The term $\rho \partial \psi / \partial \xi$ establishes an energetic penalty for large concentrations and forces the vacancies to diffuse towards a uniform state. The term $e z \phi$ accounts for electrostatic interactions due to charges of the vacancies, and leads to their migration towards locations where the potential ϕ is small. The final distribution of vacancies is thus established from a balance of the contributions of these two terms in the chemical potential.

6. Conclusions

A continuum model for elastic dielectric semiconductors with mobile charged point vacancies has been presented. The complete 3-D theoretical framework includes the physics of continuum elasticity, electrostatics, mass diffusion, and charged defect kinetics.

A restricted version of the theory has been implemented in a finite difference code allowing solution of the elliptic equations of electrostatics of dielectrics coupled with the transient parabolic equation of charged diffusion. The numerical analysis is at present limited to one spatial dimension.

User documentation has been provided for the computer implementation. Given in the report are descriptions of the source code structure, user instructions, and representative input files for analysis of BST thin films containing charged oxygen vacancies. The source code has been included in the appendix.

7. References

- Buchanan, D. A. *IBM J. Res. Develop.* **1999**, *43*, 245.
- Carnahan, B.; Luther, H. A.; Wilkes, J. O. *Applied Numerical Methods*; Wiley: New York, 1969.
- Chapra, S. C.; Canale, R. P. *Numerical Methods for Engineers with Programming and Software Applications*; 3rd ed.; McGraw-Hill: Boston, 1998.
- Cole, M. W.; Nothwang, W. D.; Hubbard, C.; Ngo, E.; Ervin, M. *J. Appl. Phys.* **2003**, *93*, 9218.
- Damjanovic, D. *Rep. Prog. Phys.* **1998**, *61*, 1267.
- Devonshire, A. F. *Phil. Mag.* **1954**, *3*, 85.
- Fried, V.; Hamerka, H. F.; Blukis, U. *Physical Chemistry*; Macmillan: New York, 1977.
- Grinfeld, M. A.; Hazzledine, P. M. *Europhys. Lett.* **1997**, *37*, 409.
- Hoffman, J. D. *Numerical Methods for Engineers and Scientists*; McGraw-Hill: Boston, 1992.
- Johnson, K. M. *J. Appl. Phys.* **1962**, *33*, 2826.
- Lifshitz, I. M. *Sov. Phys. JETP*, **1963**, *17*, 909.
- Stratton, J. A. *Electromagnetic Theory*; McGraw-Hill: New York, 1941.
- Tinte, S.; Stachiotti, M. G.; Phillpot, S. R.; Sepiarsky, M.; Wolf, D.; Migoni, R. L. *J. Phys. Condens. Matter* **2004**, *16*, 3495.
- Todd, S. S.; Lorenson, R. E. *J. Amer. Chem. Soc.* **1952**, *74*, 2043.
- Toupin, R. A. *J. Rat. Mech. Anal.* **1956**, *5*, 849.
- Zafar, S.; Jones, R. E.; Jiang, B.; White, B.; Chu, P.; Taylor, D.; Gillespie, S. *Appl. Phys. Lett.* **1998**, *73*, 175.

Appendix. Source Code

This appendix appears in its original form, without editorial change.

INTENTIONALLY LEFT BLANK.

```

program semiconductor_1D
c
implicit none
c
character(len=50) problem_type
c
integer i,j,k,l,m,n
integer nmax !max # of nodes in grid
integer nsteps !max * of timesteps
integer nout,kount,count !# steps between output requests
integer ke,kc !output flags
c
real*8 t,tmax,dt !time,max time, delta-time
real*8 p1,p2 !permittivity constants
real*8 d1,d2 !bulk diffusivity constants
real*8 z !valence per vacancy
real*8 temp !temperature (K)
real*8 alpha !convert to per m^3 from ppm
real*8 beta !convert to vol. fraction from ppm
real*8 L0,LC !initial and current domain length (m)
real*8 Ldot !velocity of domain (m/s)
real*8 dx !grid spacing (m)
real*8 x !coordinate (nm)
real*8 pfree !permittivity of free space (C/Vm)
real*8 kb !Boltzmann's constant (J/K)
real*8 e !charge of an electron (C)
real*8 s !specific entropy (J/molK)
real*8 cp !specific heat (J/molK)
real*8 cave0 !initial avg concentration (ppm)
real*8,pointer,dimension(:)::dconc !cumulative change in conc (ppm)
real*8,pointer,dimension(:)::dconst !relative dielectric constant
real*8,pointer,dimension(:)::efield !electric field (V/m)
real*8,pointer,dimension(:)::potential !electric potential (V)
real*8,pointer,dimension(:)::charge !electric charge (C)
real*8,pointer,dimension(:,)::earray !electric field output matrix
real*8,pointer,dimension(:,)::carray !concentration output matrix
c
500 format(12e14.5)
c
pfree = 8.854187817d-12
kb = 1.3806505d-23
e = 1.60217653d-19
c
open(unit=1,file='parameters.inp',status='unknown')
read(1,*)problem_type
read(1,*)nmax
read(1,*)tmax
read(1,*)dt
read(1,*)nout
read(1,*)L0
read(1,*)temp
read(1,*)p1
read(1,*)p2
read(1,*)d1
read(1,*)d2
read(1,*)alpha
read(1,*)beta

```

```

read(1,*)z
read(1,*)s
read(1,*)cp
close(1)

c
print*, 'Problem ', problem_type
print*, 'Domain initial length ', L0
print*, 'Number of nodes ', nmax
print*, 'Max time and delta_t ', tmax, dt
print*, 'Bulk diffusion constants ', d1, d2
print*, 'Bulk dielectric constants ', p1, p2
print*, 'Valence per vacancy ', z
print*, 'Temperature ', temp
print*, 'Entropy ', s
print*, 'Specific heat', cp
print*, 'Conversion ppm to per cubic meter ', alpha
print*, 'Conversion ppm to volume fraction ', beta

c
nsteps= tmax/dt
nsteps= nsteps/nout+1
print*, 'Number of output steps ', nsteps

c
allocate(dconc(nmax))
allocate(dconst(nmax))
allocate(efield(nmax))
allocate(potential(nmax))
allocate(charge(nmax))
allocate(earray(nmax, nsteps))
allocate(carray(nmax, nsteps))

c
t=0.0
do i=1, nmax
dconc(i)=0.0
dconst(i)=p1
efield(i)=0.0
potential(i)=0.0
charge(i)=0.0
end do
do i=1, nmax
do j=1, nsteps
earray(i, j)=0.0
carray(i, j)=0.0
end do
end do

Ldot=0.0
LC=L0
kount=nout
count=nout
ke=0
kc=0

c
100 if(t.le.tmax) then
c
dx=LC/(nmax-1.)
c

```

```

        if(problem_type.eq.'maxwell')then
        call elliptic(dconc,dx,temp,p1,p2,z,e,charge,dt,pfree,
1             alpha,t,dconst,nmax,efield,potential,
2             nout,count,tmax,earray,nsteps,ke)
        end if
c
        if(problem_type.eq.'fick')then
        call parabolic(dconc,dconst,d1,d2,temp,nmax,dx,Ldot,s,cp,
1 beta,t,dt,z,e,kb,pfree,alpha,efield,charge,potential,tmax,
2 nout,kount,cave0,carray,nsteps,kc)
        end if
c
        if(problem_type.eq.'mixed')then
        call elliptic(dconc,dx,temp,p1,p2,z,e,charge,dt,pfree,
1             alpha,t,dconst,nmax,efield,potential,
2             nout,count,tmax,earray,nsteps,ke)
c
        call parabolic(dconc,dconst,d1,d2,temp,nmax,dx,Ldot,s,cp,
1 beta,t,dt,z,e,kb,pfree,alpha,efield,charge,potential,tmax,
2 nout,kount,cave0,carray,nsteps,kc)
        end if
c
        t = t + dt
        LC = LC+(Ldot*dt)
        go to 100
        end if
c
        open(unit=5,file='earray.txt',status='unknown')
        open(unit=6,file='carray.txt',status='unknown')
        x=0.0
        do i=1,nmax
        write(5,500)x,(earray(i,j),j=1,nsteps)
        write(6,500)x,(carray(i,j),j=1,nsteps)
        x=x+dx*1.0d9
        end do
        close(5)
        close(6)
c
        deallocate(dconc)
        deallocate(dconst)
        deallocate(efield)
        deallocate(potential)
        deallocate(charge)
        deallocate(earray)
        deallocate(carray)
c
        end program semiconductor_1D
c
c#####
c
        subroutine elliptic(dconc,dx,temp,p1,p2,z,e,charge,dt,
1             pfree,alpha,t,dconst,nmax,efield,potential,
2             nout,count,tmax,earray,nsteps,ke)
c
        implicit none
c
        character(len=50)bcleft,bcright,dummychar

```

```

integer i,j,k,l,m,n
integer nmax,adim,nout,count,nsteps,ke
integer,pointer,dimension(:)::index
real*8 dx,temp,p1,p2,z,e,pfree,alpha,t,dt,tmax,tout
real*8 valleft,valright
real*8 dconc(nmax)
real*8 dconst(nmax)
real*8 charge0(nmax)
real*8 charge(nmax)
real*8 potential(nmax)
real*8 efield(nmax)
real*8 x(nmax)
real*8 earray(nmax,nsteps)
real*8 factor,energy,d
real*8,pointer,dimension(:,:)::amatrix
real*8,pointer,dimension(:)::bvector
real*8,pointer,dimension(:)::xvector
200 format(i6,5e14.5)
c
open(unit=2,file='electrostatic.inp',status='unknown')
read(2,*)bcleft
read(2,*)valleft
read(2,*)bcright
read(2,*)valright
read(2,*)dummychar
do i=1,nmax
    read(2,*)charge0(i)
end do
close(2)
c
adim=nmax
c
if(bcleft.eq.'potential')then
    adim=adim-1
end if
c
if(bcright.eq.'potential')then
    adim=adim-1
end if
c
allocate(amatrix(adim,adim))
allocate(bvector(adim))
allocate(xvector(adim))
allocate(index(adim))
c
do i=1,nmax
    charge(i)=charge0(i)+e*z*dconc(i)*alpha
    x(i)=dfloat(i-1)*dx
end do
c
do i=1,adim
    do j=1,adim
        amatrix(i,j)=0.0
    end do
    amatrix(i,i)=-2.0
    k=i+1
    m=i-1

```

```

if(i.lt.adim)amatrix(i,k)=1.0
if(i.gt.1)amatrix(i,m)=1.0
end do
c
factor=-dx*dx/pfree
do i=1,adim
j=i
if(bcleft.eq.'potential')j=j+1
bvector(i)=charge(j)*factor/dconst(j)
end do
c
if(bcleft.eq.'potential') bvector(1)=bvector(1)-valleft
c
if(bcrightright.eq.'potential')then
bvector(adim)=bvector(adim)-valright
end if
c
if(bcleft.eq.'flux') then
bvector(1)=bvector(1)-2.*valleft*dx
amatrix(1,2)=2.0
end if
c
if(bcrightright.eq.'flux') then
bvector(adim)=bvector(adim)+2.*valright*dx
i=adim-1
amatrix(adim,i)=2.0
end if
c
call LU_Decomp(adim,amatrix,index)
call LU_BackSub(adim,amatrix,index,bvector)
c
do i=1,adim
j=i
if(bcleft.eq.'potential')then
potential(1)=valleft
j=i+1
end if
potential(j)=bvector(i)
if(bcrightright.eq.'potential') potential(nmax)=valright
end do
c
k=nmax-1
do i=2,k
j=i-1
m=i+1
efield(i)=(potential(j)-potential(m))/(2.*dx)
end do
efield(1)=(potential(1)-potential(2))/dx
efield(nmax)=(potential(k)-potential(nmax))/dx
if(bcleft.eq.'flux')efield(1)=valleft
if(bcrightright.eq.'flux')efield(nmax)=valright
c
energy=0.0
do i=1,k
energy=energy+dconst(i)*efield(i)*efield(i)*dx
end do
c

```

```

d=energy*dx*dfloat(nmax-1)/(potential(1)-potential(nmax))**2.
c
do i=1,nmax
dconst(i)=p1/((1.+p2*efield(i)*efield(i))**(0.333333333))
end do
c
tout=tmax-dt
c
if(count.eq.nout.or.t.gt.tout)then
ke=ke+1
count=0
if(t.lt.dt)then
open(unit=3,file='outelec.txt',
1 status='unknown')
else
open(unit=3,file='outelec.txt',position='append',
1 status='unknown')
end if
do i=1,nmax
write(3,200)i,t,x(i),potential(i),efield(i),charge(i)
earray(i,ke)=efield(i)/1.0d5
end do
close(3)
print*,'Effective dielectric constant ',d
end if
c
count=count+1
c
deallocate(amatrix)
deallocate(bvector)
deallocate(xvector)
deallocate(index)
c
return
end
c
c-#####
c
subroutine parabolic(dconc,dconst,d1,d2,temp,nmax,dx,Ldot,s,cp,
1 beta,t,dt,z,e,kb,pfree,alpha,efield,charge,potential,tmax,
2 nout,kount,cave0,carray,nsteps,kc)
c
implicit none
c
character(len=50)bcleft,bcright,constraint
integer i,j,k,l,m,n
integer nmax,nout,kount,nsteps,kc
real*8 dconc(nmax)
real*8 dconst(nmax)
real*8 efield(nmax),charge(nmax),potential(nmax)
real*8 d1,d2,temp,dx,t,dt,z,e,kb,pfree,beta
real*8 alpha,Ldot,s,cp,tmax,tout
real*8 valleft,valright
real*8 conc0(nmax)
real*8 conc(nmax)
real*8 cdot(nmax),gradc(nmax)
real*8 diff1(nmax),diff2(nmax),q(nmax),x(nmax)

```

```

real*8 denom,phi,dphi
real*8 c,cdotmax,cdottemp,cave,cave0,L0,LC
real*8 test,scale
real*8 carray(nmax,nsteps)
300 format(i6,5e14.5)
c
open(unit=4,file='diffusion.inp',status='unknown')
read(4,*)bcleft
read(4,*)valleft
read(4,*)bcright
read(4,*)valright
read(4,*)constraint
do i=1,nmax
read(4,*)conc0(i)
end do
close(4)
c
if(t.eq.0.0)then
cave0=0.0
L0=0.0
do i=1,nmax
cave0=cave0+dx*conc0(i)
L0=L0+dx
end do
cave0=cave0/L0
end if
c
test = 1./6.*dx*dx/(d1*kb*temp)
c if(dt.gt.test)print*,'Warning: dt may be unstable!',test
c
do i=1,nmax
x(i)=dfloat(i-1)*dx
conc(i)=conc0(i)+dconc(i)
c=conc(i)
call chem_potential(c,temp,kb,alpha,s,cp,phi,dphi)
diff1(i)=-d1*dphi
diff2(i)=d2*e*z*efield(i)
end do
c
k=nmax-1
do i=2,k
m=i+1
n=i-1
gradc(i)=(diff1(m)-diff1(n))/(2.*dx)
q(i)= gradc(i)+diff2(i)
end do
c
if(bcleft.eq.'potential')then
gradc(1)=(-3.*diff1(1)+4.*diff1(2)-diff1(3))/(2.*dx)
q(1)= gradc(1)+diff2(1)
end if
c
if(bcright.eq.'potential')then
i=nmax-1
j=nmax-2
gradc(nmax)=(3.*diff1(nmax)-4.*diff1(i)+diff1(j))/(2.*dx)
q(nmax)= gradc(nmax)+diff2(nmax)

```

```

end if
c
if(bcleft.eq.'flux')q(1)=valleft
if(bcrightright.eq.'flux')q(nmax)=valright
c
if(bcleft.eq.'special')then
c=conc(1)
call chem_potential(c,temp,kb,alpha,s,cp,phi,dphi)
q(1)=valleft/(1.-conc(1)*beta)*
1 (phi+potential(1)*charge(1)+0.5*efield(1)*efield(1)
2 *dconst(1)*pfree+(1./beta-conc(1))*dphi/beta+e*z*potential(1)*
3 (1.-conc(nmax)*beta))
end if
c
if(bcrightright.eq.'special') then
c=conc(nmax)
call chem_potential(c,temp,kb,alpha,s,cp,phi,dphi)
q(nmax)=valright/(1.-conc(nmax)*beta)*(phi+potential(nmax)*
1 charge(nmax)+0.5*efield(nmax)*efield(nmax)*dconst(nmax)*pfree
2 +(1./beta-conc(nmax))*dphi/beta+e*z*potential(nmax)*
3 (1.-conc(nmax)*beta))
end if
c
k=nmax-1
do i=2,k
m=i+1
n=i-1
cdot(i)=-((q(m)-q(n))/(2.*dx))
end do
c
cdot(1)=-((-3.*q(1)+4.*q(2)-q(3))/(2.*dx))
i=nmax-1
j=nmax-2
cdot(nmax)=-((3.*q(nmax)-4.*q(i)+q(j))/(2.*dx))
c
if(bcleft.eq.'potential')cdot(1)=0.0
if(bcrightright.eq.'potential')cdot(nmax)=0.0
c
do i=1,nmax
cdottemp=cdot(i)
conc(i)=conc(i)+cdot(i)*dt
if (conc(i).lt.1.d-15)cdot(i)=0.0
conc(i)=conc(i)-cdottemp*dt
end do
c
if (constraint.eq.'yes')then
cave=0.0
LC=0.0
do i=1,nmax
dconc(i)=dconc(i)+cdot(i)*dt
cave=cave+(conc0(i)+dconc(i))*dx
LC=LC+dx
end do
cave=cave/LC
scale=cave0/cave
do i=1,nmax
dconc(i)=dconc(i)*scale-conc0(i)*(1.-scale)

```



```

subroutine chem_potential(c,temp,kb,alpha,s,cp,phi,dphi)
c
  implicit none
c
  real*8 c,temp,kb,alpha,cp,s,phi,dphi
  real*8 gtotal
  real*8 xv
  real*8 avagadro,r
  real*8 nt
c
  avagadro = 6.02214199447d23
  r = 8.314472
c
  nt = alpha*1.0d6
  xv = c*alpha/nt
c
  gtotal = temp*(cp-s+r*log(xv))
c
  phi = nt/avagadro*gtotal
  dphi = kb*temp*c
  dphi = kb*temp*log(c)
c
  return
  end
c
c-#####
c
  subroutine LU_Decomp(n,a,index)
c
  implicit double precision (a-h,o-z)
  dimension a(n,n), index(n), v(n)
c
  tiny = 1.0e-20
c
  do i = 1,n
    a_max = 0.0
    do j = 1,n
      a_max = max(a_max,abs(a(i,j)))
    end do !j
    v(i) = 1.0 / a_max
  end do !i
c
  do j = 1,n
c
  do i = 1,j-1
    sum = a(i,j)
    do k = 1,i-1
      sum = sum - a(i,k) * a(k,j)
    end do
    a(i,j) = sum
  end do
c
  a_max = 0.0
  do i = j,n
    sum = a(i,j)
    do k = 1,j-1
      sum = sum - a(i,k) * a(k,j)

```

```

end do
a(i,j) = sum
dummy = v(i) * abs(sum)
if ( dummy .gt. a_max ) then
imax = i
a_max = dummy
end if
end do
c
if ( j .ne. imax ) then
do k = 1,n
dummy = a(imax,k)
a(imax,k) = a(j,k)
a(j,k) = dummy
end do
v(imax) = v(j)
end if
index(j) = imax
c
if ( a(j,j) .eq. 0.0 ) a(j,j) = tiny
if ( j .ne. n ) then
dummy = 1.0 / a(j,j)
do i = j+1,n
a(i,j) = a(i,j) * dummy
end do
end if
end do !j
c
return
end
c
c-#####
c
subroutine LU_BackSub(n,a,index,b)
c
implicit double precision (a-h,o-z)
dimension a(n,n), index(n), b(n)
c
ii = 0
c
do i = 1,n
m = index(i)
sum = b(m)
b(m) = b(i)
if ( ii .ne. 0 ) then
do j = ii,i-1
sum = sum - a(i,j) * b(j)
end do
else if ( sum .ne. 0.0 ) then
ii = i
end if
b(i) = sum
end do
c
do i = n,1,-1
sum = b(i)
if ( i .lt. n ) then

```

```
do j = i+1,n
sum = sum - a(i,j) * b(j)
end do
end if
b(i) = sum / a(i,i)
end do
c
return
end
c
c=====
```

NO. OF
COPIES ORGANIZATION

1 DEFENSE TECHNICAL
(PDF INFORMATION CTR
ONLY) DTIC OCA
8725 JOHN J KINGMAN RD
STE 0944
FORT BELVOIR VA 22060-6218

1 US ARMY RSRCH DEV &
ENGRG CMD
SYSTEMS OF SYSTEMS
INTEGRATION
AMSRD SS T
6000 6TH ST STE 100
FORT BELVOIR VA 22060-5608

1 DIRECTOR
US ARMY RESEARCH LAB
IMNE ALC IMS
2800 POWDER MILL RD
ADELPHI MD 20783-1197

3 DIRECTOR
US ARMY RESEARCH LAB
AMSRD ARL CI OK TL
2800 POWDER MILL RD
ADELPHI MD 20783-1197

ABERDEEN PROVING GROUND

1 DIR USARL
AMSRD ARL CI OK TP (BLDG 4600)

NO. OF
COPIES ORGANIZATION

38 DIR USARL
AMSRD ARL CI HC
P CHUNG
R NAMBURU
D GROVE
AMSRD ARL WM
J MCCAULEY
T WRIGHT
AMSRD ARL WM TA
S SCHOENFELD
AMSRD ARL WM TC
M FERMAN COKER
R COATES
AMSRD ARL WM TD
S BILYK
T BJERKE
D CASEM
J CLAYTON (5 CPS)
T CLINE
D DANDEKAR
W EDMANSON
M GREENFIELD
C GUNNARSSON
Y HUANG
K IYER
R KRAFT
B LOVE
S MCNEILL
H MEYER
R MUDD
M RAFTENBERG
E RAPACKI
M SCHEIDLER
S SEGLETES
T WEERASOORIYA
AMSRD ARL WM MA
M COLE
J ANDZELM
M VANLANDINGHAM
W NOTHWANG
AMSRD ARL WM MD
G GAZONAS